Priority Brief

Cancer Immunology Research

PD-L1 Antibodies to Its Cytoplasmic Domain Most Clearly Delineate Cell Membranes in Immunohistochemical Staining of Tumor Cells

Kathleen M. Mahoney[1,2], Heather Sun[3], Xiaoyun Liao[1,4], Ping Hua[1], Marcella Callea[3], Edward A. Greenfield[1], F. Stephen Hodi[1,4], Arlene H. Sharpe[5], Sabina Signoretti[3], Scott J. Rodig[3,4], and Gordon J. Freeman[1]

Abstract

Blocking the programmed death-1 (PD-1) pathway has clinical benefit in metastatic cancer and has led to the approval of the mAbs pembrolizumab and nivolumab to treat melanoma and nivolumab for non–small cell lung cancer. Expression of PD-L1 on the cell surface of either tumor cells or infiltrating immune cells is associated with a higher likelihood of response to PD-1 blockade in multiple studies. Most mAbs to PD-L1 in use are directed to its extracellular domain and immunohistochemically stain tumor tissue with a mixture of cytoplasmic and membrane staining. Cytoplasmic staining obscures the interpretation of a positive reaction on the tumor cell membrane, and thus affects the accuracy of PD-L1 scoring systems. We developed a mAb to the cytoplasmic domain of PD-L1, 405.9A11 (9A11), which is both more selective for membranous PD-L1 and more sensitive in IHC and Western blotting, compared with previous mAbs specific for the PD-L1 extracellular domain. Here, we compare immunohistochemical staining patterns of PD-L1 expression in five types of tumors, using five PD-L1 mAbs: 9A11, 7G11, and three commercially available mAbs. We demonstrate that 9A11, as well as two other cytoplasmic domain-specific mAbs, E1L3N and SP142, can clearly delineate the membrane of PD-L1–positive cells in formalin-fixed paraffin-embedded tissue and facilitate interpretation of staining results. *Cancer Immunol Res; 3(12); 1308–15. ©2015 AACR.*

Introduction

The programmed death-1 [PD-1 (CD273, B7-DC)] pathway is a critical immune checkpoint regulating peripheral tolerance. PD-1 is a B7/CD28 superfamily receptor expressed on activated and exhausted T cells, as well as some activated B cells, dendritic cells (DC), and monocytes. PD-1 negatively regulates lymphocyte function through signaling triggered by engagement with its ligands, PD-L1 (CD274, B7-H1), and PD-L2 (CD273, B7-DC), as documented in refs. 1–3. The PD-1 pathway downregulates the intensity and duration of immune responses. PD-L1 is expressed on many hematopoietic cells, including DCs, macrophages, mesenchymal stem cells, and bone marrow–derived mast cells (4), and is induced on activated T cells. PD-L1 also can be inducibly expressed on epithelial and endothelial cells by IFNs and is constitutively expressed on some cells at sites of immune privilege such as syncytiotrophoblasts in the placenta and in the retina. Expression of PD-L1 on nonhematopoietic cells plays a role in peripheral T-cell tolerance (reviewed in ref. 5).

Therapeutic blockade of either PD-1 or PD-L1 produces impressive antitumor responses in phase I, II, and III clinical trials in multiple tumor types. This has led to FDA accelerated approval of the PD-1 antibodies pembrolizumab and nivolumab for melanoma and non–small cell lung cancer (NSCLC). In addition, nivolumab has breakthrough designation for Hodgkin lymphoma and atezolizumab (MPDL3280A, a PD-L1 antibody) has breakthrough designation for bladder cancer and NSCLC (6–8). Many other tumor types also have increased expression of PD-L1, including nasopharyngeal, ovarian, breast and renal cell carcinomas (RCC; refs. 3, 9–12). Expression of PD-L1 on tumors facilitates immune evasion and also increases tumorigenesis and invasiveness *in vivo*. In some tumors such as RCC and ovarian carcinoma, increased expression of PD-L1 on the tumor is associated with poor prognosis (11, 13).

PD-L1 expression can be induced by IFNs, but PD-L1 expression on epithelial and hematopoietic tumor cells also may be a consequence of genomic alterations in the tumor. PD-L1 may be induced in tumors by various oncogene pathways, such as activated JAK2 or EGFR, or loss of Pten or LKB1. Constitutive PD-L1 expression caused by chromosomal amplification produces a homogeneous expression pattern, as seen in the malignant cells of Hodgkin lymphoma with the PD-L1, 405.9A11 (9A11) mAb (14). PD-L1 expression also can be induced in tumors by IFNγ made by infiltrating T cells. In some tumors, this can be seen as

[1]Department of Medical Oncology, Dana-Farber Cancer Institute, Harvard Medical School, Boston, Massachusetts. [2]Division of Hematology and Oncology, Beth Israel Deaconess Medical Center, Harvard Medical School, Boston, Massachusetts. [3]Department of Pathology, Brigham and Women's Hospital, Harvard Medical School, Boston, Massachusetts. [4]Center for Immuno-Oncology, Dana-Farber Cancer Institute, Harvard Medical School, Boston, Massachusetts. [5]Department of Microbiology and Immunobiology, Harvard Medical School, Boston, Massachusetts.

Note: Supplementary data for this article are available at Cancer Immunology Research Online (http://cancerimmunolres.aacrjournals.org/).

Corresponding Author: Gordon J. Freeman, Dana-Farber Cancer Institute, 450 Brookline Avenue, Boston, MA 02215. Phone: 617-632-4585; Fax: 617-632-5167; E-mail: gordon_freeman@dfci.harvard.edu

doi: 10.1158/2326-6066.CIR-15-0116

AACR

PD-L1 expression at the interface of tumor and infiltrating lymphocytes, and this feedback loop of PD-L1–mediated immune evasion has been termed adaptive resistance (15). The mechanism directing PD-L1 expression likely influences the pattern of its expression in the tumor. Heterogeneity of PD-L1 expression has been seen in many tumors, including NSCLC and RCC (16, 17).

Early studies of clinical correlations described distinct patterns of PD-L1 tumor expression by immunohistochemical staining (IHC), including cytoplasmic, membranous, or absent expression (6, 18). Expression of membranous PD-L1 on tumors has been associated with higher response rates to PD-1 checkpoint blockade with the PD-1 antibodies nivolumab and pembrolizumab (10, 16). One of the limitations of PD-L1 IHC is the difficulty in distinguishing membranous from cytoplasmic staining. Further work is needed to compare the value of PD-L1 as a biomarker across treatments and among PD-L1 mAb used in predictive companion IHC assays that are being developed in parallel with each pharmaceutical company's PD-1/PD-L1 treatment antibody. The sensitivity and specificity of a mAb for its target protein affects how PD-L1 expression is scored. Improved reagents for defining PD-L1 expression within the tumor may better distinguish patterns of expression within the tumor and better determine its role as a predictive biomarker for response to treatment.

We have developed mAbs to detect PD-L1 in flow cytometry, Western blot, and immunohistochemical analyses. PD-L1 is a protein with seven exons encoding 5′ untranslated, secretory signal, IgV, IgC, 11 amino acid stalk plus transmembrane, cytoplasmic 1, and cytoplasmic 2 exons with a stop codon followed by a 3′ untranslated and poly(A) tail. The majority of this transmembrane protein is extracellular, including the PD-1–binding domain, but PD-L1 also has a short 31 amino acid cytoplasmic domain. We have mAbs that recognize distinct domains within PD-L1 (IgV, IgC, and cytoplasmic). In the first-in-human phase I report of nivolumab, the IHC staining of tumor cells with the 5H1 mAb was described as membranous, cytoplasmic, or no PD-L1 staining in formalin-fixed, paraffin-embedded (FFPE) tissue (12, 18, 19). We also found similar patterns of staining with both the 015 and 7G11 mAbs. The 5H1, 015, and 7G11 mAbs all bind the extracellular domain of PD-L1. We found the mixture of cytoplasmic and membranous staining with the 7G11 and 015 mAbs sometimes difficult to interpret, thus we focused on developing a mAb with a more selective PD-L1 membranous staining pattern to facilitate analysis of tumor specimens in an automated assay. We describe here IHC with three PD-L1 mAbs specific for the PD-L1 cytoplasmic domain (9A11, E1L3N, and SP142) that give clear membranous staining. We show that the PD-L1 cytoplasmic domain-specific mAb 9A11 is highly sensitive and specific for Western blot analysis and IHC of PD-L1.

Materials and Methods

Cell lines

HDLM2, L428, and OC1-LY1 hematologic cell lines were a gift of Dr. Margaret Shipp (Dana-Farber Cancer Institute, Boston, MA), and were cultured as described previously (12). Caki-2 (ATCC), SKBR3 (ATCC), and SKOV3 (ATCC) cells were maintained in McCoy's 5A media-10% FBS, glutamine, and antibiotics as recommended by the ATCC. UMRC6 cells were maintained in DMEM-10%FBS/pen-strep/glutamine/HEPES/gentamycin, and SN12C, BT474 (ATCC), and MDA-MB-231 (ATCC) cells without HEPES. OVCAR5 cells were maintained in DMEM-10% FBS/pen-strep/non-essential amino acids. 769-P (ATCC), 36M2 and A2780-C70 cells were maintained in RPMI-10%FBS/pen-strep. Kidney cancer cell lines were a gift of Drs. Chuan Shen and William Kaelin (Dana-Farber Cancer Institute). Ovarian cell lines were a gift of Dr. Panos Konstantinopoulos (Dana-Farber Cancer Institute). Cell lines from the ATCC were authenticated at the ATCC by short tandem repeat profiling and maintained in culture for less than 6 months. Lymphoid and kidney cell lines were authenticated by expression of cell surface lineage markers, but no further authentication was performed. Adherent epithelial cell lines (renal, breast, and ovarian lines) were passed by trypsinization; however, for flow cytometry and protein lysate preparation, cells were detached from plastic with 1 mmol/L EDTA-PBS to minimize cleavage of extracellular protein domains. PD-L1–transfected 300.19 cell lines were used for controls and were previously described (3).

PD-L1 mAbs

PD-L1 mAbs that recognize the cytoplasmic domain of human PD-L1 protein were generated by immunizing BALB/c PD-L1$^{-/-}$ mice with a 19-mer peptide having the sequence, CGIQDTNSKKQSDTHLEET, which represents the last 19 amino acids at the carboxy-terminus of the human membrane-bound PD-L1 polypeptide. Mice were immunized i.p. with 100 μg of peptide coupled to Keyhole limpet hemocyanin (KLH) in complete Freund's adjuvant. At 2 week intervals for four more times, the mice were immunized i.p with 100 μg of peptide-KLH in incomplete Freund's adjuvant. Twenty-four days after the last immunization, the mouse was given 50 μg of peptide coupled to BSA by the i.v. route. Four days later, the spleen and lymph nodes were harvested and used in a hybridoma fusion with SP2/0 myeloma cells. Cells were cultured in 96-well plates and assayed by ELISA on peptide-BSA and by Western blot analysis on lysates of untransfected and human PD-L1–transfected 300.19 cells.

Clone 405.9A11 (9A11, mouse IgG1, and Kappa) was chosen for further analysis based on its capacity to Western blot human PD-L1 and detect PD-L1 expression by flow cytometry of permeabilized PD-L1–transfected 300.19 cells. Clones 29E.2A3 (mouse IgG2b, Kappa), 339.7G11 (7G11) and 368A.5A4 (5A4; both mouse IgG1, Kappa) have been previously described (1, 12) and recognize an epitope in the PD-L1 IgV domain. E1L3N and SP142 (both rabbit IgG) are mAbs directed against the PD-L1 cytoplasmic domain were from Cell Signaling Technology and Spring Bioscience, respectively. Clone 015 (rabbit IgG) directed against the PD-L1 extracellular domain was from Sino Biologicals.

Flow cytometry

Cells from culture were suspended in flow cytometry wash buffer (PBS/2%FBS/0.02% sodium azide/0.5mmol/L EDTA) to minimize clumping of epithelial cells. Primary and secondary antibodies were added at 10 μg/mL working concentration; isotype controls included MOPC-21 (mIgG1), C1.18.4 (mIgG2a), and MPC.11 (mIgG2b). After a 30-minute incubation on ice, cells were washed twice and incubated with goat anti-mouse IgG antibody conjugated to PE (Southern Biotech) for 30 minutes on ice. Cells were washed twice and resuspended in 2% formalin in PBS and stored at 4°C until analyzed on a Canto II cytometer. Flow-cytometry data were analyzed with FlowJo software.

Western blot analysis

Protein lysates were prepared with RIPA buffer per the manufacturer's instructions (Thermo Fisher Scientific), and protease inhibitor cocktail was added to the buffer (complete Ultra tablets, mini, EDTA-free, Roche) before lysate preparation. Thirty-five micrograms of lysates was loaded into a 4% to 15% gradient mini-Protean TGX gel (Bio-Rad) and transferred by a semidry method. Membranes were blocked with TBS with Tween20 (TBST) with 12% non-fat milk and 1% normal goat serum for 1 hour at room temperature. The membrane was washed with TBST and incubated with the primary antibody (final concentration of 20 μg/mL for 7G11, 10 μg/mL for 5A4, 5 μg/mL for 9A11, and 1 μg/mL for β-actin (Abcam) or 1 μg/mL 9A11, E1L3N, and SP142 in the Supplementary Figs. S1 and S2) in TBST and 1% BSA at 4°C overnight. Membranes were washed with TBST three times at room temperature and incubated with secondary antibody (1:4,000, goat anti-mouse IgG; Southern Biotech) in TBST, 6% nonfat milk and 0.5% normal goat serum for 30 minutes. After three additional washes with TBST, a 1:1 ratio of ECL substrate:enhancer was added to the membrane (SuperSignal West Pico Stable Peroxide Solution, Supersignal West Pico Luminol/Enhancer Solution; Thermo Fisher Scientific) and imaged on Hyblot CL autoradiography film (Denville Scientific).

To assess the sensitivity and affinity of the PD-L1 antibodies, 250 to 600 μg of protein lysate was run on a wide single well gel, transferred to membrane, mounted in a multichannel cassette (Immunetics), and the indicated dilutions (concentrations of 20, 5, 1.25, 0.31, or 0.078 μg/mL) of mAb were loaded in adjacent channels. A detection mixture of 1:4,000 of both goat anti–mouse-IgG-HRP and goat anti–rabbit-IgG-HRP antibodies (Santa Cruz Biotechnology) was used.

Immunohistochemistry

All staining used 4-μm-thick FFPE tissue sections. The blocks ranged from <1 to 13 years in age. After staining, slides were washed, dehydrated, and coverslipped. IHC using clone 015 rabbit anti-human PD-L1 mAb (6.2 μg/mL final concentration; Sino Biological), and 7G11 mouse anti-human PD-L1 monoclonal antibody (mAb; IgG1, 69 μg/mL final concentration; ref. 12) was performed on a Benchmark XT autostainer (Ventana Medical System) with standard antigen retrieval (CC1 buffer, pH 8.0; Ventana). The UltraView Universal DAB Detection Kit (Ventana) was used according to the manufacturer's instruction. Counterstaining was performed as part of the automated staining protocol using hematoxylin (Ventana).

IHC using clone 9A11 mouse anti-human PD-L1 mAb (IgG1, 10.4 μg/mL final concentration) was performed on a Bond III automated staining system (Leica Biosystems) following the manufacturer's protocol. Slides were loaded onto a Leica Bond III instrument with "Bond Universal Covertiles" (Leica Biosystems). PD-L1 (9A11) immunostaining was performed using Discovery Ab diluent (Ventana). Heat-induced antigen retrieval was performed using ER2 solution (pH8; Leica) for 30 minutes. Primary antibody was incubated for total of 2 hours with two separate applications, follow by 8 minutes of postprimary blocking reagent, 12 minutes of horseradish peroxidase–labeled polymer, 5 minutes of peroxidase block, 15 minutes of 3,3′-diaminobenzidine (DAB) developing, and 10 minutes of hematoxylin staining. All reagents were components of the Bond Polymer Refine detection system (Leica). IHC using the E1L3N rabbit anti-human PD-L1 mAb (Cell Signaling Technology) was performed by the same protocol as 9A11 (final concentration: 5.4 μg/mL) using Bond Primary Antibody Diluent.

IHC using clone SP142 rabbit anti-human PD-L1 mAb (IgG, 0.7 μg/mL final concentration) was performed using the manufacturer's manual protocol with antigen retrieval in EDTA buffer pH8.0, with steamer/boiling.

Evaluation of immunohistochemical staining

Reactivity for PD-L1 was determined by two blinded pathologists. Discrepant results in staining interpretation (<5% of cases) were resolved in a consensus conference. We have extensive experience in staining PD-L1 in tumors (12, 14, 17) and selected PD-L1$^+$ tumors to compare IHC expression patterns of PD-L1 between tumor types using the 5 different PD-L1 mAbs. For each stained slide, the percentage of tumor cells and pattern of PD-L1 staining on tumor cells and non-malignant immune cells was reported as cytoplasmic (C), membranous (M), or nuclear. The percentage of tumor cells showing positive staining for PD-L1 with each of the mAbs was recorded as 0, <5, 5, 10, and greater than 10 in 10% increments (0%–100%). A representative PD-L1$^+$ case of each tumor type was selected for staining and quantification. In addition, the intensity of positive staining on tumor cells, nonmalignant immune infiltrate, and the extracellular matrix was recorded: (−), no staining detected; (1+), weak staining; (2+), moderate staining; (3+), strong staining.

Results and Discussion

Western blot analysis with anti–PD-L1 mAbs

The development of PD-L1 mAbs for IHC of FFPE tissues has been difficult due to the mix of membranous and cytoplasmic staining observed with several PD-L1 mAb (12, 18, 20). Several pharmaceutical companies have developed PD-L1 mAbs for IHC; however, direct comparisons have been limited as these antibodies are proprietary (16, 21, 22). We previously reported that 7G11 and 015 antibodies can detect PD-L1 in FFPE specimens (12) and showed a staining pattern similar to that previously described with the 5H1 antibody: membranous and cytoplasmic expression (18). Multiple other PD-L1 mAbs work poorly or not at all in IHC with high background (20). Previously reported mAbs recognize a determinant in the extracellular domain, and could also detect PD-L1 intracellular stores or splice variants retained in the cytoplasm. PD-L1 splice variants that have the extracellular domain but lack the cytoplasmic domain are present in Genbank. The expression of such PD-L1 splice variants might contribute to the cytoplasmic staining. Whether these PD-L1 splice variants are secreted, accumulate intracellularly, or are unstable and degraded is currently not known. We reasoned that a mAb specific for the cytoplasmic domain would enforce detection of full-length PD-L1 protein and might give more selective membranous staining, facilitating the measurement of tumor cell PD-L1 expression. In addition, a cytoplasmic domain–specific mAb can be used for analysis of PD-L1 expression even in the presence of a PD-L1 therapeutic mAb.

We immunized PD-L1–deficient mice with a PD-L1 cytoplasmic domain peptide and generated an mAb, 9A11, that recognizes the human PD-L1 cytoplasmic domain. Initial screening of the antibody was performed by intracellular flow cytometry, Western blot analysis, and IHC of human PD-L1–transfected

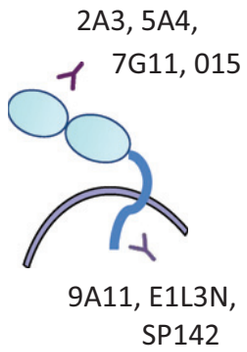

Figure 1.
Domain specificity of PD-L1 mAbs. 9A11, E1L3N, and SP142 recognize an epitope in the cytoplasmic domain of PD-L1, whereas most other mAbs used for therapeutics, flow cytometry, and IHC recognize an epitope in the extracellular domain of PD-L1, including 2A3, 5A4, 7G11, and 015.

and –untransfected cells (Supplementary Fig. S3 and data not shown). We compared 9A11 with previously generated mAbs against the PD-L1 extracellular domain and cytoplasmic domain (Fig. 1) to compare their sensitivity and specificity for detecting endogenous levels of native human PD-L1 in Western blots of human tumor cell lines. To compare antibody affinities, we performed dose curves of each cytoplasmic domain antibody in a multichannel cassette Western blot analysis of protein lysates from HDLM2 Hodgkin lymphoma, Caki-2 kidney, and SKBR3 breast cancer cell lines. We found 9A11 to be more sensitive than E1L3N and SP142 in Western blot analysis (Fig. 2A). We also performed dose curves of 7G11 and 015 alongside 5A4, 9A11, and E1L3N (Supplementary Fig. S1). The 5A4 antibody had the highest affinity in Western blot format, detecting PD-L1 robustly at 0.31 μg/mL. 9A11 had the second highest affinity, declining at 0.31 μg/ml. E1L3N declined at 1.25 μg/mL, whereas 015 and 7G11 only worked modestly at 5 and 20 μg/mL, respectively. The relative sensitivity of these mAbs in Western blot format was 5A4 > 9A11 > SP142 = EIL3N >> 015 > 7G11.

We found that 9A11 is more specific than 7G11 and as specific as 5A4 for the full-length PD-L1 protein in Western blot analysis of human cell lines (Fig. 2B). 9A11, E1L3N, and SP142 Western blotted only a single band at the expected size of the mature PD-L1 protein (approximately 50 kDa; Supplementary Fig. S2). Although unglycosylated PD-L1 is expected to be about 23 kDa, mature PD-L1 is expected to be 45 to 55 kDa when fully glycosylated at all 4 N-linked glycosylation sites. The molecular weight was consistently slightly higher (55 kDa) in epithelial cell lines and lower in the Hodgkin lymphoma cell lines (51.5 kDa), perhaps due to the complexity of glycosylation. Although 5A4 detects PD-L1 by Western blot and flow cytometry, it does not work in IHC. In addition, 7G11 also detected several lower MW bands, ranging from 35 to 45 kDa, which may be alternative splice variants, proteins that share similarity to the recognized PD-L1 epitope, or a consequence of having to use relatively higher concentrations of 7G11 in Western blots.

Detection of PD-L1 by Western blot analysis correlated with its surface expression by flow cytometry

The 29E.2A3 antibody, which recognizes the IgV domain of PD-L1, is highly sensitive for PD-L1 in flow cytometry but does not work in Western blots. It has been used to show PD-L1 expression on Hodgkin lymphoma cell lines (HDLM2 and L428) and breast cancer cell lines (MDA231 and SKBR3; refs. 3, 9, 12), and the absence of PD-L1 on the diffuse large B-cell lymphoma OC1-Ly1 and BT474 breast cancer cell lines by flow cytometry (3, 9). We found that one of four RCC cell lines (Caki-2) and three of four ovarian cancer cell lines (36M2, OVCAR5, and SKOV3) examined

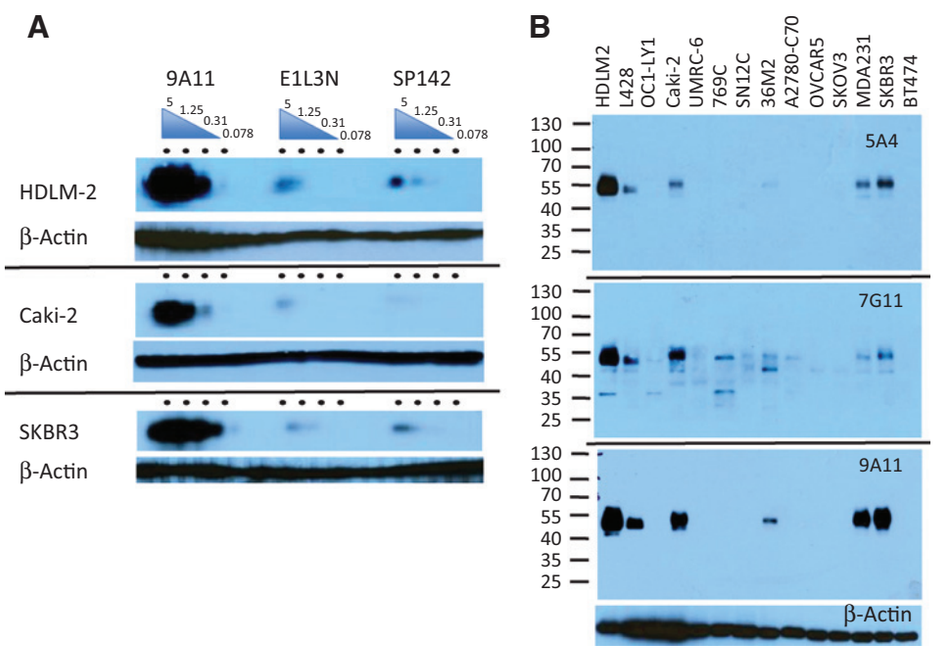

Figure 2.
Western blotting of PD-L1 mAbs. A, multichannel Western blot analysis with dose curve of each antibody (5, 1.25, 0.31, and 0.078 μg/mL per lane) on HDLM2, Caki-2, or SKBR3, as indicated. Blot was developed with an equal mixture of anti-mouse and anti-rabbit IgG-HRP antibodies. B, Western blot analysis of hematologic (HDLM2, L428, and OC1-LY1), kidney (Caki-2, UMRC-6, 769C, and SN12C), ovarian (36M2, A2780-C70, and OVCAR3), and breast cancer cell lines (MDA231, SKBR3, and BT474) with anti–PD-L1 mAbs: 5A4 (10 μg/mL), 7G11 (20 μg/mL), 9A11 (5μg/mL), or anti–β-actin A and B are representative of two to five experiments.

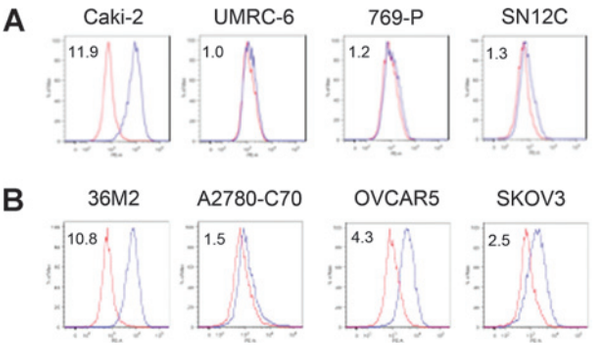

Figure 3.
Flow cytometry of kidney (A) and ovarian (B) tumor cell lines with PD-L1 mAb (2A3). Representative of three experiments.

express PD-L1 on their surface by flow cytometry (Fig. 3). Flow cytometry with the 2A3 mAb appears to have somewhat greater sensitivity than Western blot with 9A11 for PD-L1 (Figs. 2B and 3). Although bands are seen in the OVCAR5 and SKOV3 lysates with 7G11 by Western blot analysis, it is unclear whether these are specific for the full-length PD-L1.

9A11 detects cell surface expression of human PD-L1 in IHC of FFPE tissue

Developing reagents for IHC in FFPE tissues can be difficult, but is important because IHC is the primary means of assaying protein expression in patient specimens. We previously reported that the 7G11 and 015 antibodies can detect PD-L1 in FFPE specimens (12) and showed a staining pattern of membranous and cytoplasmic PD-L1 expression (18). We compared the ability of five different mAbs with PD-L1, 9A11, 7G11, E1L3N, 015, and SP142 to detect PD-L1 expression in FFPE specimens by IHC on an automated platform in a series of different tumor types: Hodgkin lymphoma, diffuse large B-cell lymphoma (DLBCL), nasopharyngeal carcinoma (NPC), NSCLC, and RCC.

Classical Hodgkin lymphoma (cHL) is an excellent example of immune evasion through high expression of PD-L1 by malignant cells (14). The malignant cells of cHL, the Reed-Sternberg cells, and primary mediastinal large B-cell lymphoma (MLBCL) cells, can express high PD-L1 and PD-L2 through gene amplification of the 9p24.1 region encoding the adjacent PD-L1 and PD-L2 genes (9). In addition, the amplicon includes the neighboring Janus kinase 2 (JAK2) gene, which confers additional responsiveness to IFN-γ mediated upregulation of PD-L1 and PD-L2 (9). All five PD-L1 mAbs stain the membrane of 90% to 100% of the Reed-Sternberg cells with high intensity (Fig. 4; Supplementary Table S1). Staining of the Reed-Sternberg cells with 7G11 and 015 was somewhat difficult to discriminate due to the marked cytoplasmic staining of the surrounding cells. With less cytoplasmic staining with 9A11, E1L3N, and SP142, it is easier to distinguish the membranous staining of the Reed-Sternberg cells and some of the PD-L1–positive immune infiltrate surrounding the cHL.

A series of DLBCLs did not express PD-L1 by flow cytometry, in contrast with the robust expression by Hodgkin lymphoma lines (9). Consistent with this, we found that PD-L1 was not detectable in Western blots of the DLBCL cell line OC-1LY-1 (Fig. 2). DLBCL tumors proved to be a good negative control for 9A11, E1L3N, and SP142 staining as the IHC analysis showed no membranous staining and little to no cytoplasmic staining (Fig. 4). 9A11 also had the lowest background in comparison with isotype control (Supplementary Fig. S4). We did observe some cytoplasmic staining in 80% of DLBCL tumor cells with 015 and less with 7G11 (Supplementary Table S1). This cytoplasmic staining pattern may be nonspecific or recognition of a shared epitope with other proteins in the tumor.

PD-L1 expression has been seen in many virally associated malignancies, including NPC, EBV-positive posttransplant lymphoproliferative lymphoma, EBV-associated DLBCL, and HHV8-associated primary effusion lymphoma (12). All five PD-L1 mAbs showed high-intensity membranous and cytoplasmic staining in 100% of NPC cells with equivalent staining intensity (Supplementary Table S1). However, they showed staining of adjacent stromal cells with an order of staining intensity of 015 > 7G11 > E1L3N > SP142 > 9A11 (Fig. 4). These results show that 9A11 gave the most intense membranous staining with little cytoplasmic staining of the NPC tumor and that E1L3N and SP142 were also excellent. When comparing PD-L1 IHC of NPC with isotype controls (Supplementary Fig. S4), the mouse isotype control for 9A11 of the same concentration appears to have less cytoplasmic staining of the adjacent stromal cells than the rabbit isotype control for E1L3N, which suggests that the cytoplasmic staining of the stroma with E1L3N is nonspecific. The uniform expression of PD-L1 in NPC is mediated by EBV LMP1 protein and PD-L1 expression can be independently upregulated further by IFNγ (23). Patients with PD-L1–positive, viral antigen–expressing tumors are anticipated to be excellent candidates for PD-1 blockade immunotherapy (reviewed in ref. 24).

The PD-L1 staining within the NSCLC and RCC tumor cells was more heterogeneous than the uniform expression seen in Hodgkin lymphoma and NPC (16, 17). Analysis of NSCLC and RCC tumor cells found the intensity of PD-L1 staining to be generally higher in NCSLS (3+) than RCC (2+), but showed similar patterns of staining with the five PD-L1 mAbs. Heterogenous PD-L1 expression in these tumors may be a consequence of adaptive resistance, whereas uniform expression may be mediated by viral oncogenes or genomic amplification. The analysis of RCC and NSCLC illustrates how when there is high cytoplasmic PD-L1 staining, as seen with 015 and 7G11, discriminating PD-L1 membranous staining of tumor cells may be less accurate. E1L3N appears to be the most sensitive for membranous PD-L1 in IHC, when comparing the percentage of PD-L1–positive tumor cells in adjacent sections of the tumor stained with mAbs that target the cytoplasmic tail of PD-L1. As shown in Supplementary Table S1, the RCC tumor had 50%, 20%, or 5% PD-L1–positive tumors cells and the NSCLC tumor had 20%, 15%, and 10% PD-L1–positive tumor cells with E1L3N, 9A11, and SP142, respectively.

Translational relevance of PD-L1 mAb comparison

The role of PD-L1 as a predictive biomarker for response to PD-1 pathway blockade has garnered much attention since an initial small study suggested its correlation with response. Additional clinical correlative studies have shown that PD-L1 expression enriches for response, but because a proportion of the PD-L1–negative group also responds, lack of PD-L1 expression fails to be a biomarker for exclusion from therapy (25). PD-L1 expression on tumor cells, as assayed with the 5H1 and 28-8 PD-L1 mAbs, is associated with response to PD-1 blockade

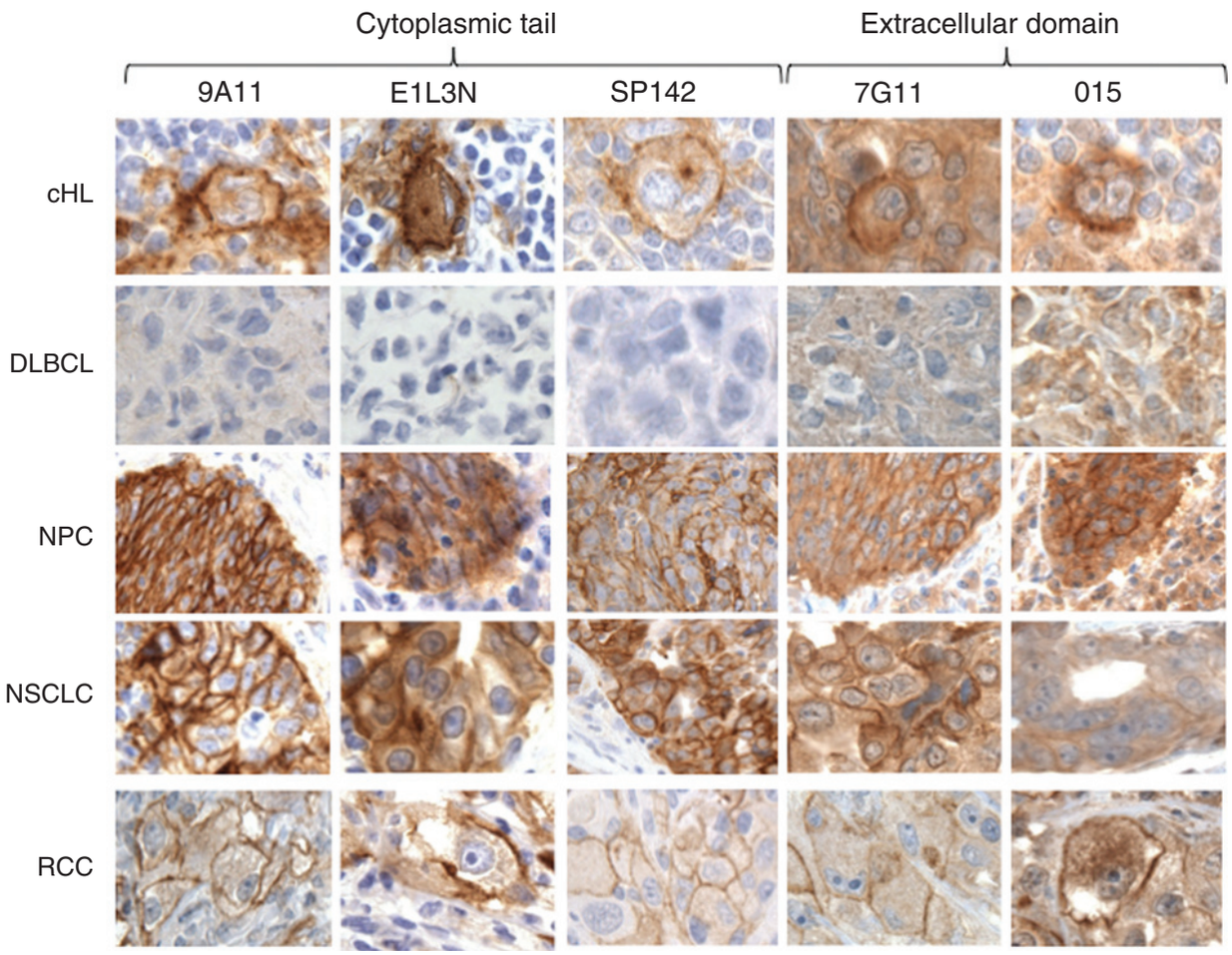

Figure 4.
Comparison of PD-L1 mAbs in IHC across multiple tumor types. Representative photomicrographs of select tumors stained with PD-L1 antibodies, 9A11, 7G11, E1L3N, 015, and SP142 (brown coloration) in cHL, DLBCL, NPC, NSCLC (a representative adenocarcinoma), and RCC, as indicated. Representative of 50 to 300 cases for 9A11, 7G11, E1L3N, and 015, and 11 cases for SP142.

with nivolumab (10, 18). In contrast, response to the PD-L1 mAb, atezolizumab, was associated with PD-L1 expression on the immune infiltrate as assayed with the SP142 PD-L1 mAb (26). Additional studies with distinct PD-L1 mAbs, 22C3 and SP263, have been presented as companions with the PD-1 blocker, pembrolizumab, and PD-L1 blocker, MEDI4736, respectively (16, 22). In later studies with each of these proprietary mAbs, a fraction of PD-L1 "negative" tumors respond. Whether these differences in response are caused by tumor heterogeneity, sensitivity of a given antibody or differences in the biology of antitumor responses between PD-1– and PD-L1–blocking antibodies has yet to be clarified. More recent work combining PD-L1 expression with other markers such as CD8 infiltrate has improved the predictive power of the assays in a multivariate model (27).

As illustrated in the NSCLC and RCC cases in this study, the threshold for "positive" expression of a protein is dependent on the sensitivity of the antibody in a given IHC protocol. More sensitive mAbs would potentially reduce the number of false-negative PD-L1 specimens, thus improving the negative predictive power of the biomarker. E1L3N may be slightly more sensitive than 9A11 in IHC, yet the isotype control for E1L3N has a higher background than the isotype control for 9A11. As we develop machine quantitated IHC, weighing the sensitivity and specificity of an antibody for its intended target protein will be important.

Here, we show somewhat different patterns of PD-L1 expression by IHC using antibodies directed against the extracellular or cytoplasmic domains of PD-L1. A membranous pattern of PD-L1 expression is best delineated with antibodies directed against the cytoplasmic tail, 9A11, E1L3N, and SP142. These three mAbs recognize an epitope in the last 19 amino acids of the PD-L1 cytoplasmic domain as measured by ELISA with BSA-conjugated peptide (Mahoney; unpublished results). The 9A11 antibody is also highly sensitive and specific for full-length PD-L1 in Western blot analysis and correlates with surface expression of PD-L1 in the same cell lines by flow cytometry. 9A11, E1L3N, and SP142 have lower backgrounds, most evident in the IHC of DLBCL. The higher backgrounds with 7G11 and 015 suggest that they lack the specificity necessary for stringent analysis of cell surface PD-L1 expression on the tumor by IHC. The functional significance of cytoplasmic expression of PD-L1 remains unclear and further

work is needed to determine whether it is a biologically significant source of PD-L1.

The similar IHC pattern with multiple PD-L1 mAbs specific for the cytoplasmic domain supports our hypothesis that targeting this domain improves the detection of PD-L1 with good selectivity for membrane localization. Distinguishing PD-L1 on tumor cells versus infiltrating immune cells may be a means to define distinct groups of tumors with different likelihoods of response to PD-1 pathway blockade. Stringent validation of reagents in automated assays will allow development of better prognostic and predictive algorithms for characterizing patterns of PD-L1 expression, be it membranous or cytoplasmic, homogeneous, or heterogeneous within tumors and infiltrating immune cells.

Disclosure of Potential Conflicts of Interest

F.S. Hodi is a consultant in Merck, reports receiving a commercial research grant from Bristol-Myers Squibb to institution, and reports receiving other commercial research support from Genentech clinical trial support to institution, Merck clinical trial support to institution, and Bristol-Myers Squibb clinical trial support to institution. A.H. Sharpe has ownership interest (including patents) in Bristol-Myers Squibb, Merck, Boehringer Ingelheim, MedImmune, Amplimmune, Novartis, Pfizer, and Genentech, and is a consultant/advisory board member for Novartis and Surface Oncology. S.J. Rodig has ownership interest (including patents) in Patent. G.J. Freeman has ownership interest (including patents) in Merck, Bristol-Myers Squibb, Roche, EMD Serono, Amplimmune, Boehringer Mannheim, and Novartis, and is a consultant/advisory board member for Novartis, Roche, Bristol-Myers Squibb, Eli Lilly, and Surface Oncology. No potential conflicts of interest were disclosed by the other authors.

Authors' Contributions

Conception and design: K.M. Mahoney, S.J. Rodig, G.J. Freeman
Development of methodology: X. Liao, S. Signoretti, S.J. Rodig
Acquisition of data (provided animals, acquired and managed patients, provided facilities, etc.): K.M. Mahoney, P. Hua, E.A. Greenfield, F.S. Hodi, S.J. Rodig, G.J. Freeman
Analysis and interpretation of data (e.g., statistical analysis, biostatistics, computational analysis): K.M. Mahoney, F.S. Hodi, A.H. Sharpe, S. Signoretti, S.J. Rodig, G.J. Freeman
Writing, review, and/or revision of the manuscript: K.M. Mahoney, X. Liao, F.S. Hodi, A.H. Sharpe, S. Signoretti, S.J. Rodig, G.J. Freeman
Administrative, technical, or material support (i.e., reporting or organizing data, constructing databases): H. Sun, P. Hua, S.J. Rodig
Study supervision: S.J. Rodig, G.J. Freeman
Other (immunohistochemical data interpretation and material support): M. Callea

Grant Support

This study was supported by DF/HCC Kidney Cancer SPORE P50CA101942 (to S. Signoretti, A.H. Sharpe, and G.J. Freeman), U54CA163125, and P01AI056299 (to G.J. Freeman and A.H. Sharpe); Claudia Adams Barr Program for Innovative Cancer Research, 2014 AACR Basic Cancer Research Fellowship, grant number 14-40-01-MAHO, and the ASCO Young Investigator Award supported by Kidney Cancer Association (to K.M. Mahoney); the Center for Immuno-Oncology, Dana-Farber Cancer Institute (to F.S. Hodi and S.J. Rodig).

The costs of publication of this article were defrayed in part by the payment of page charges. This article must therefore be hereby marked *advertisement* in accordance with 18 U.S.C. Section 1734 solely to indicate this fact.

Received April 27, 2015; revised August 24, 2015; accepted September 8, 2015; published OnlineFirst November 6, 2015.

References

1. Brown JA, Dorfman DM, Ma FR, Sullivan EL, Munoz O, Wood CR, et al. Blockade of programmed death-1 ligands on dendritic cells enhances T-cell activation and cytokine production. J Immunol 2003;170:1257–66.
2. Freeman GJ, Long AJ, Iwai Y, Bourque K, Chernova T, Nishimura H, et al. Engagement of the PD-1 immunoinhibitory receptor by a novel B7 family member leads to negative regulation of lymphocyte activation. J Exp Med 2000;192:1027–34.
3. Latchman Y, Wood CR, Chernova T, Chaudhary D, Borde M, Chernova I, et al. PD-L2 is a second ligand for PD-1 and inhibits T-cell activation. N Immunol 2001;2:261–8.
4. Yamazaki T, Akiba H, Iwai H, Matsuda H, Aoki M, Tanno Y, et al. Expression of programmed death 1 ligands by murine T cells and APC. J Immunol 2002;169:5538–45.
5. Sharpe AH, Wherry EJ, Ahmed R, Freeman GJ. The function of programmed cell death 1 and its ligands in regulating autoimmunity and infection. Nat Immun 2007;8:239–45.
6. Topalian SL, Hodi FS, Brahmer JR, Gettinger SN, Smith DC, McDermott DF, et al. Safety, activity, and immune correlates of anti–PD-1 antibody in cancer. N Engl J Med 2012;366:2443–54.
7. Hamid O, Robert C, Daud A, Hodi FS, Hwu WJ, Kefford R, et al. Safety and tumor responses with lambrolizumab (anti–PD-1) in Melanoma. N Engl J Med 2013;369:134–144.
8. Hamid O, Sosman JA, Lawrence DP, Sullivan RJ, Ibrahim N, Kluger HM, et al. Clinical activity, safety, and biomarkers of MPDL3280A, an engineered PD-L1 antibody in patients with locally advanced or metastatic melanoma (mM). J Clin Oncol 2013;31:(suppl; abstr 9010).
9. Green MR, Monti S, Rodig SJ, Juszczynski P, Currie T, O'Donnell E, et al. Integrative analysis reveals selective 9p24.1 amplification, increased PD-1 ligand expression, and further induction via JAK2 in nodular sclerosing Hodgkin lymphoma and primary mediastinal large B-cell lymphoma. Blood. 2010;116:3268–77.
10. Taube JM, Klein AP, Brahmer JR, Xu H, Pan X, Kim JH, et al. Association of PD-1, PD-1 ligands, and other features of the tumor immune microenvironment with response to anti–PD-1 therapy. Clin Cancer Res 2014;20:5064–74.
11. Thompson RH, Gillett MD, Cheville JC, Lohse CM, Dong H, Webster WS, et al. Costimulatory B7-H1 in renal cell carcinoma patients: indicator of tumor aggressiveness and potential therapeutic target. Proc Natl Acad Sci U S A 2004;101:17174–9.
12. Chen BJ, Chapuy B, Ouyang J, Sun HH, Roemer MG, Xu ML, et al. PD-L1 expression is characteristic of a subset of aggressive B-cell lymphomas and virus-associated malignancies. Clin Cancer Res 2013;19:3462–73.
13. Hamanishi J, Mandai M, Iwasaki M, Okazaki T, Tanaka Y, Yamaguchi K, et al. Programmed cell death 1 ligand 1 and tumor-infiltrating $CD8^+$ T lymphocytes are prognostic factors of human ovarian cancer. Proc Natl Acad Sci U S A 2007;104:3360–5.
14. Ansell SM, Lesokhin AM, Borrello I, Halwani A, Scott EC, Gutierrez M, et al. PD-1 blockade with nivolumab in relapsed or refractory Hodgkin's lymphoma. N Engl J Med 2015;372:311–9.
15. Taube JM, Anders RA, Young GD, Xu H, Sharma R, McMiller TL, et al. Colocalization of inflammatory response with B7-h1 expression in human melanocytic lesions supports an adaptive resistance mechanism of immune escape. Sci Translat Med 2012;4:127ra37.
16. Garon EB, Rizvi NA, Hui R, Leighl N, Balmanoukian AS, Eder JP, et al. Pembrolizumab for the treatment of non–small cell lung cancer. N Engl J Med 2015;372:2018–28.
17. Callea M, Albiges L, Gupta M, Cheng SC, Genega EM, Fay AP, et al. Differential expression of PD-L1 between primary and metastatic sites in clear cell renal cell carcinoma. Cancer Immunol Res 2015;3:1158–64.
18. Brahmer JR, Drake CG, Wollner I, Powderly JD, Picus J, Sharfman WH, et al. Phase I study of single-agent anti-programmed death-1 (MDX-1106) in

refractory solid tumors: safety, clinical activity, pharmacodynamics, and immunologic correlates. J Clin Oncol 2010;28:3167–75.
19. Dong H, Zhu G, Tamada K, Chen L. B7-H1, a third member of the B7 family, co-stimulates T-cell proliferation and interleukin-10 secretion. Nat Med 1999;5:1365–9.
20. Gadiot J, Hooijkaas AI, Kaiser AD, van Tinteren H, van Boven H, Blank C. Overall survival and PD-L1 expression in metastasized malignant melanoma. Cancer 2011;117:2192–201.
21. Wolchok JD, Kluger H, Callahan MK, Postow MA, Rizvi NA, Lesokhin AM, et al. Nivolumab plus ipilimumab in advanced melanoma. N Engl J Med 2013;369:122–133.
22. Segal NH, Antonia SJ, Brahmer JR, Maio M, Blake-Haskins A, Li X, et al. Preliminary data from a multi-arm expansion study of MEDI4736, an anti–PD-L1 antibody. J Clin Oncol 2014;32:5s:(suppl; abstr 3002^).
23. Fang W, Zhang J, Hong S, Zhan J, Chen N, Qin T, et al. EBV-driven LMP1 and IFN-gamma up-regulate PD-L1 in nasopharyngeal carcinoma: implications for oncotargeted therapy. Oncotarget 2014;5: 12189–202.
24. Ott PA, Hodi FS. The B7-H1/PD-1 pathway in cancers associated with infections and inflammation: opportunities for therapeutic intervention. Chin Clin Oncol 2013;2:7.
25. Mahoney KM, Atkins MB. Prognostic and predictive markers for the new immunotherapies. Oncology 2014;28:39–48.
26. Herbst RS, Soria JC, Kowanetz M, Fine GD, Hamid O, Gordon MS, et al. Predictive correlates of response to the anti–PD-L1 antibody MPDL3280A in cancer patients. Nature 2014;515:563–7.
27. Tumeh PC, Harview CL, Yearley JH, Shintaku IP, Taylor EJ, Robert L, et al. PD-1 blockade induces responses by inhibiting adaptive immune resistance. Nature 2014;515:568–71.